applied sciences

MDPI

Article

On the Anticoagulant Activities of Acidic Polysaccharides from the Western Mediterranean Sea Porifera

Tiziana Cubeddu [1], Gabriele Costa [2], Gabriele Nieddu [3], Paolo Mereu [3], Nicola Fois [2], Renata Manconi [1,*], Marilena Formato [3] and Antonio Junior Lepedda [3,*]

[1] Department of Veterinary Medicine, University of Sassari, Via Vienna 2, 07100 Sassari, Italy; tcubeddu@uniss.it
[2] AGRIS-Sardegna, Agricultural Research Agency of Sardinia, Bonassai, 07100 Sassari, Italy; gabrielec1987@gmail.com (G.C.); nfois@agrisricerca.it (N.F.)
[3] Department of Biomedical Sciences, University of Sassari, Viale San Pietro 43b, 07100 Sassari, Italy; ganieddu@uniss.it (G.N.); pmereu@uniss.it (P.M.); formato@uniss.it (M.F.)
* Correspondence: renata.manconi@gmail.com (R.M.); ajlepedda@uniss.it (A.J.L.); Tel.: +39-079-228606 (A.J.L.)

Featured Application

Porifera harbor an evolutionarily conserved family of bioactive molecules with a remarkable ability to modulate hemostasis. Combined with the feasibility of rearing these organisms in an environmentally sustainable manner, fully aligned with blue economy principles, our findings identify these acidic polysaccharides as strong candidates for next-generation anticoagulant therapeutics, with potential extending to regenerative medicine and tissue engineering.

Abstract

Innovation in the field of bioinspired therapeutic anticoagulants, as an alternative to heparin and its derivatives, is increasingly focused toward the discovery of new molecules from natural sources. Inspired by the compelling observation that marine organisms possess a wide array of acidic polysaccharides (APs) within their extracellular matrix (ECM) with promising anticoagulant potential, this study investigates AP topographic distribution, content, and bioactivity in the body of seven phylogenetically distant Mediterranean sponge species. Tissue architecture was evidenced by Alcian Blue histological staining whereas biochemical analyses were carried out on APs purified from papain-digested tissue extracts using anion-exchange chromatography. Four polysaccharide fractions were obtained and assessed for hexuronic acid content. The two most abundant ones, up to 98% of the total, were characterized by electrophoretic analyses, and assessed *in vitro* for inhibitory activity on blood coagulation. Histology evidenced a heterogeneous distribution of APs within the sponge's ECM, along with marked interspecific variability in both concentration and electrophoretic profiles. Neither *Tethya aurantium* nor *Crambe crambe* showed any significant in vitro effects on coagulation, whereas the other species exhibited a strong inhibitory effect on both activated partial thromboplastin time (aPTT) and thrombin time (TT), comparable to standard heparin (Hep). Concerning aPTT, both *I. retidermata* and *H. communis* reached the endpoint of 300 s at 5 µgUA/mL, whereas *S. spinosulus*, *O. lobularis*, *A. aerophoba* reached it at 10 µgUA/mL. With reference to TT, *A. aerophoba*, *I. retidermata*, *S. spinosulus* and *H. communis* had comparable effects on coagulation time with respect to Hep (endpoint at 5 µgUA/mL), whereas *O. lobularis* was less effective (endpoint at 100 µgUA/mL). These findings show that Porifera, one of the most basal Metazoa, have an ECM rich in APs with anticoagulant properties towards both intrinsic and common pathways of coagulation, consistent with known inhibitory mechanisms reported for certain marine sulfated polysaccharides derived from other invertebrate taxa. These molecules, obtainable

Check for updates

Academic Editor: Adina Magdalena Musuc

Received: 20 March 2026
Revised: 17 April 2026
Accepted: 20 April 2026
Published: 22 April 2026

Copyright: © 2026 by the authors. Licensee MDPI, Basel, Switzerland. This article is an open access article distributed under the terms and conditions of the Creative Commons Attribution (CC BY) license.

through sustainable blue technology, represent compelling candidates for bioinspired next-generation anticoagulant therapeutics, with broader applications in regenerative medicine and tissue engineering.

Keywords: marine natural products; next-generation anticoagulants; Mediterranean Sea sponges; marine molecular biodiversity

1. Introduction

Heparin and its derivatives remain core anticoagulants, yet their clinical utility is significantly constrained by both bleeding and non-bleeding toxicities [1,2]. Major bleeding represents the primary safety concern associated with unfractionated heparin (UFH) or low-molecular-weight heparin (LMWH) administration; however, clinically significant adverse effects extend well beyond hemorrhage, encompassing heparin-induced thrombocytopenia, osteoporosis, cutaneous hypersensitivity, alopecia, eosinophilia, and endocrine dysfunctions [2–4]. Furthermore, UFH exhibits considerable pharmacokinetic variability arising from extensive non-specific binding to plasma and cellular proteins. This unpredictability necessitates continuous therapeutic monitoring and frequent dosage adjustments. Thus, recent years have seen an intensified interest in identifying alternative therapeutic anticoagulants from natural sources, particularly marine organisms, which may offer superior safety profiles and strong anticoagulant potency due to their unique chemical structures and biological activities [5]. This approach bridges biomedical advancement with environmental responsibility, aiming to improve patient outcomes while promoting the sustainable use of marine biodiversity within the framework of the blue economy.

In this respect, anticoagulant activity has been documented for fucoidan isolated from holothurians [6] and seaweeds [7], as well as for fucosylated chondroitin sulfate (FCS), which has been identified exclusively in the body wall of holothurians, so far [8]. Notably, a FCS-derived nonasaccharide has been shown to selectively modulate the intrinsic coagulation pathway by binding to FIXa and disrupting FIXa–FVIIIa interactions. This mechanism is associated with reduced risk of bleeding compared to traditional heparinoids and warfarin [9], highlighting its potential as a promising alternative to conventional anticoagulant therapies. Beyond echinoderms and macroalgae, marine sponges represent a further yet underexplored source of structurally diverse extracellular matrix (ECM) polysaccharides. As basal metazoans, sponges possess a collagen-rich ECM containing complex polysaccharides, which has attracted increasing attention for bioinspired biomedical applications [10–12]. Hence, sustainable sponge marine culture systems represent an environmentally compatible platform to produce bioactive compounds with low ecological impact [13]. Recently, a highly charged polysaccharide was isolated [14] from the marine sponge *Sarcotragus spinosulus* Schmidt, 1862. This compound demonstrated in vitro anticoagulant properties and cytocompatibility, with infrared spectroscopy and nuclear magnetic resonance revealing structural similarities with the FCS purified from the sea cucumber *Holothuria* (*Holoturia*) *tubulosa* Gmelin, 1791 [14]. The biotechnological application of these natural anticoagulants has also been explored in vascular tissue engineering. In particular, these polysaccharides were exploited to functionalize nanofibrous poly(ε-caprolactone) electrospun scaffolds, thus conferring both anticoagulant and antiplatelet aggregation properties as well as enhanced endothelialization to the synthetic matrix [15,16].

Prompted by the observation that the simplest metazoans, i.e., Porifera, bear in their ECMs acidic polysaccharides (APs) physiologically involved in cell–cell crosstalk [17–19] and potentially useful as anticoagulants in some biomedical applications [15,16], in the

present study, a screening of Mediterranean sponge species was performed, evaluating both quali-quantitatively and functionally different polysaccharide fractions. Interestingly, five out of the seven experimental models were found to be rich in APs with strong anticoagulant activity compared with heparin (Hep), evaluated by activated partial thromboplastin time (aPTT), prothrombin time (PT), and thrombin time assays.

2. Materials and Methods

All reagents and chemicals used in this study were of analytical grade from Merck Group (KGaA, Darmstadt, Germany), unless otherwise specified.

2.1. Experimental Models Species

Representative specimens of seven phylogenetically distant Mediterranean Porifera species, namely *Oscarella lobularis* (Schmidt, 1862), *Tethya aurantium* (Pallas, 1766), *Crambe crambe* (Schimdt, 1862), *Ircinia retidermata* Pulitzer-Finali & Pronzato, 1981, *Sarcotragus spinosulus* Schmidt, 1862, *Hippospongia communis* (Lamarck, 1814) and *Aplysina aerophoba* (Nardo, 1833), were selected as experimental models (Table 1). They were cultured and collected from a sustainable, shallow water experimental sponge mariculture plant [20,21] located in the Tramariglio Cove (40°35′32.47″ N 8°10′11.50″ E, Capo Caccia—Isola Piana Marine Protected Area, northwestern Sardinian Sea, Western Mediterranean) (Figures 1 and 2). The species investigated belong to two classes, three subclasses, five orders, six families and seven genera.

Table 1. Porifera species selected as experimental models.

Class	Order	Family	Genus	Species
Homoscleromorpha	Homosclerophorida	Oscarellidae	*Oscarella*	*Oscarella lobularis* (Schmidt, 1862)
Demospongiae	Tethyida	Tethyidae	*Tethya*	*Tethya aurantium* (Pallas, 1766)
Demospongiae	Poecilosclerida	Crambeidae	*Crambe*	*Crambe crambe* (Schmidt, 1862)
Demospongiae	Dictyoceratida	Irciniidae	*Ircinia*	*Ircinia retidermata* Pulitzer-Finali & Pronzato, 1981
Demospongiae	Dictyoceratida	Irciniidae	*Sarcotragus*	*Sarcotragus spinosulus* Schmidt, 1862
Demospongiae	Dictyoceratida	Spongiidae	*Hippospongia*	*Hippospongia communis* (Lamarck, 1814)
Demospongiae	Verongiida	Verongidae	*Aplysina*	*Aplysina aerophoba* (Nardo, 1833)

Sponges are filter feeders pumping a huge amount of water through inhalant/exhalant canals (aquiferous system), and filter the water by specialized flagellated cells (choanocites) of the choanosome. The selected species are widespread inhabitants of Mediterranean coastal waters on rocky substrates, seagrass meadows and caves, mostly in shaded habitats. Growth morph ranges from encrusting with lobed surface (*O. lobularis*, *C. crambe*), to massive with lobes (*I. retidermata*, *S. spinosulus*, and *H. communis*), up to tubular-arborescent (*A. aerophoba*) or spherical in *T. aurantium* (Figures 1 and 2). They produce a huge array of metabolites and macromolecules, including steroids, lipids, alkaloids, peptides, polysaccharides, and sulfated polysaccharides, also involved in chemical defense and ecological interactions [11,12,14,22–27].

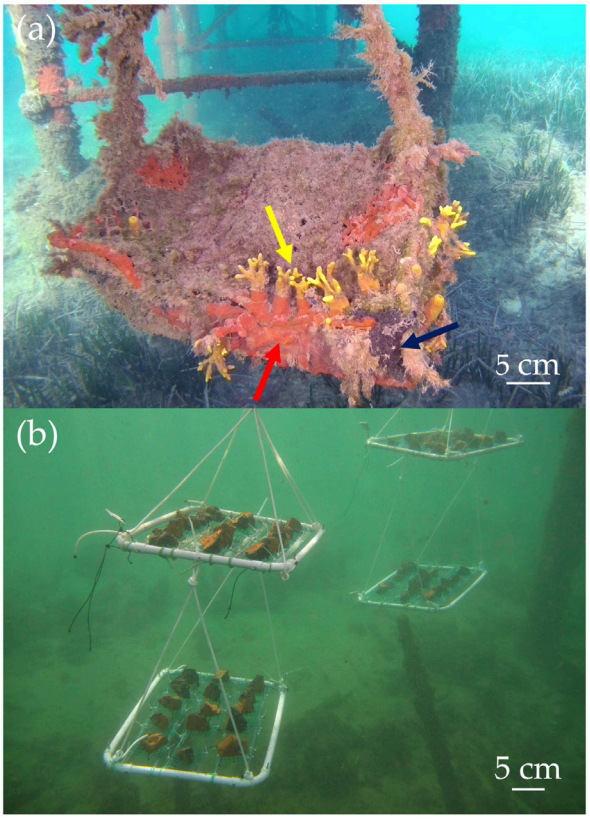


Figure 1. Representative Porifera model species grown in the experimental sponge-culture plant (Sardinian Sea, Tramariglio Cove). (**a**) *Oscarella lobularis* (encrusting dark blue, blue arrow), *Aplysina aerophoba* (arborescent yellow, yellow arrow), and *Crambe crambe* (encrusting red, red arrow), cultured in a box. (**b**) *Sarcotragus spinosulus* cultured in square frames.

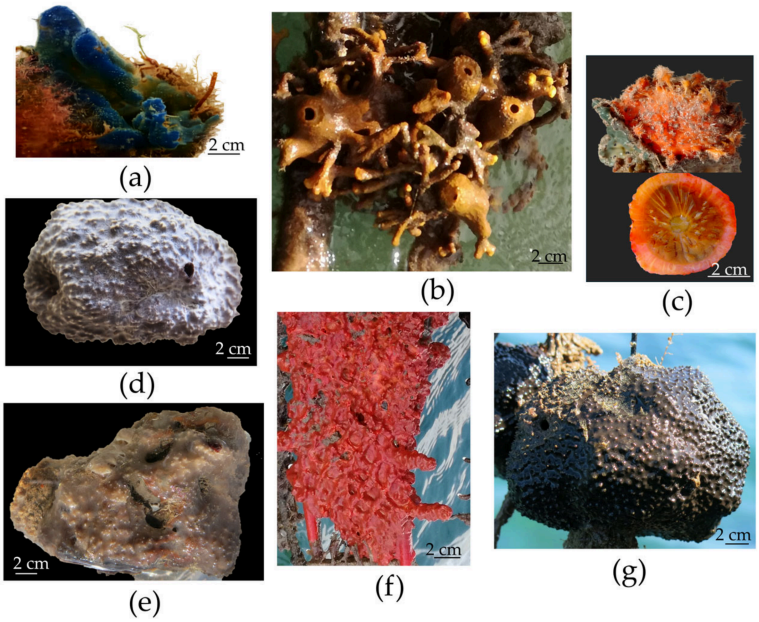


Figure 2. Macroscopic view of the seven Mediterranean sponge species selected as experimental models. (**a**) *Oscarella lobularis*; (**b**) *Aplysina aerophoba*; (**c**) *Tethya aurantium* (top) and its body cross-section (bottom) with cortex (outer layer) and medulla (inner layer); (**d**) *Ircinia retidermata*; (**e**) *Hippospongia communis*; (**f**) *Crambe crambe*; (**g**) *Sarcotragus spinosulus*.

2.2. Histological Analyses

Representative body fragments of each species were collected from experimental mariculture clonal sponges by means of a scalpel [20,21]. Samples were kept in sea water, in refrigerated bags, until analysis. For downstream histological evaluation, several fragments were fixed at room temperature for 48 h in Bouin's fluid, dehydrated in ascending ethanol series up to 100%, cleared in xylene, and embedded in paraffin. Sections 5 µm thick were stained with Alcian blue (pH 2.5) to evaluate the presence and topographic distribution of APs. Slides were examined under a Nikon ECLIPSE 80i Light Microscope (Nikon Europe B.V., Amstelveen, The Netherlands), and microphotographs were taken with a Nikon Digital-Sight DS-FI camera (Nikon Europe B.V., Amstelveen, The Netherlands).

2.3. AP Purification and Characterization

AP purification and analyses were performed as previously described with slight modifications [14].

Fresh specimens of each species under study were dehydrated through absolute ethanol incubation for 120 h at 4 °C, finely minced, followed by delipidation in acetone for 24 h. After complete acetone evaporation, dehydrated and delipidated tissues (DDT) were rehydrated with 0.1 M sodium acetate buffer, pH 6.0, containing 5 mM EDTA and 5 mM cysteine (15 mL per gram of tissue) at 4 °C for 24 h, followed by proteolytic treatment with 1 U of papain per mg of DDT (Thermo Fisher Scientific Inc. Waltham, MA, USA) at 56 °C for 48 h; enzyme activity was stopped by boiling the mixture at 100 °C for 5 min. Clarified digests were recovered and immediately loaded into an anion-exchange chromatography column packed with DEAE-Sephacel resin (10 mL of resin per gram of digested tissue), previously equilibrated with 20 mM Tris-HCl buffer, pH 8.6. The same buffer was used to wash the column until absorbance at 280 nm was less than 0.05. APs were fractionated by performing four elution steps using 20 mM Tris-HCl buffer, pH 8.6, containing 0.5 M, 1 M, 1.5 M, or 2 M sodium chloride, respectively. Eluates were concentrated and dialyzed against deionized water by means of Amicon Ultra-15 Centrifugal Filter Units with a 3 kDa cut-off, according to the manufacturer's instructions (Millipore, Burlington, MA, USA).

2.3.1. Hexuronic Acid Quantification

Each eluate was assayed for hexuronic acid (UA) content by the method of Bitter and Muir, using glucuronolactone as a standard [28]. Briefly, 250 µL of either standard (from 5 to 40 µgUA/mL) or eluates were added with 1.25 mL of 25 mM sodium tetraborate decahydrate in concentrated sulphuric acid and incubated at 85 °C for 10 min for complete depolymerization. Following UA staining by adding 50 µL of 7.5 mM carbazole in absolute ethanol at 85 °C for 15 min, absorbance was read at 530 nm.

2.3.2. Carbohydrate Electrophoresis

Carbohydrate electrophoresis (C-PAGE) was carried out in a Mini Protean II cell vertical slab gel electrophoresis apparatus (Bio-Rad laboratories, Hercules, CA, USA) using 13.5% T and 3% C polyacrylamide running gels, overlaid with 5% T and 3% C stacking gel, using 40 mM acetic acid and 40 mM Tris-HCl, pH 7.8, solution as running buffer. An amount of 2.0 µg UA of each standard polysaccharide, namely high-molecular-weight hyaluronic acid (HMW-HA) sodium salt from *Streptococcus equi* (1,500,000–1,750,000 Da), dermatan sulfate (DS) and heparin (Hep) sodium salt from porcine intestinal mucosa, and a fraction of acidic polysaccharide were added with 4X loading buffer containing 250 mM Tris-HCl, pH 7.8, 40% glycerol, and 0.008% cresol red, and run at 50 V for the first 10 min and then at 120 V until the dye front reached the bottom of the gel. The run was performed at 4 °C. Afterwards, gels were stained by overnight incubation with a solution of 50%

ethanol containing 0.005% Stains-all dye, in the dark, at room temperature. Following destaining/rehydration with distilled water for 30 min, gels were acquired with a Nikon D3100 reflex camera (Nikon Europe B.V., Amstelveen, The Netherlands).

2.3.3. Depolymerization Assays

The first two fractions from each species, as well as standard GAGs, namely Hep, DS, and HMW-HA, were assessed for susceptibility to depolymerization by specific lyases, particularly chondroitin ABC lyase from *Proteus vulgaris* and hyaluronidase from bovine testes. Chondroitin ABC lyase treatment was performed in 0.1 M CH_3COONa buffer, pH 7.5, using 0.01 U/10 μgUA at 37 °C for 24 h. Hyaluronidase treatment was performed in 0.06 M CH_3COONa buffer, pH 6, using 0.1 U/10 μgUA at 37 °C for 24 h.

2.3.4. Coagulation Assays

The anticoagulant activity of the first two eluted fractions from each species was evaluated in vitro in comparison with that of standard GAGs, using commercially available kits by Siemens Healthcare GMBH (Erlangen, Germany). In particular, activated partial thromboplastin time (aPTT) (Dade® Actin® FSL), prothrombin time (PT) (Dade® Innovin®), and thrombin time (TT) (Dade® Thrombin Reagent) assays were performed to evaluate the inhibition of the intrinsic, extrinsic and common coagulation pathways, respectively. Commercial human coagulation control plasma was used for all coagulation tests. Each fraction was added to the control plasma at different UA concentrations to assess the effects of these APs on the inhibition of clot formation. The endpoint of each test was set at 300 s.

The aPTT assay was carried out according to the manufacturer's guidelines. Briefly, 100 μL of plasma, previously added with purified polysaccharides or standard GAGs, was mixed with 100 μL of prewarmed FSL reagent and incubated at 37 °C for 3 min; then, 100 μL of prewarmed 25 mM calcium chloride solution was added, and the resulting fibrin clot formation time was measured by optical detection.

The PT assay was performed following the producer's instructions, as well. In detail, 100 μL of plasma, containing purified APs or standard GAGs, was incubated at 37 °C for 1 min, and 200 μL of prewarmed Dade® Innovin® Reagent was added. Clot formation time was measured by optical detection.

The TT assay was performed following the producer's instructions, with slight modifications. A volume of 200 μL of plasma was prewarmed at 37 °C for 2 min, added with 100 μL of 1:20 diluted thrombin reagent, and the coagulation time was measured.

All measurements were carried out in triplicate, and results were reported as mean and standard deviation.

3. Results and Discussion

3.1. Histological Analysis

Alcian blue staining revealed interspecific variations in the abundance and topographic distribution of APs within the ECM of the investigated sponges (Figure 3). In most species, staining intensity followed a decreasing gradient from the outside (ectosome) toward the inside (choanosome) of the body architecture, indicating a higher concentration of APs in the outer body region.

A homogeneous distribution throughout the body architecture was observed only in *O. lobularis*, where both ectosome and choanosome exhibited comparable staining intensity.

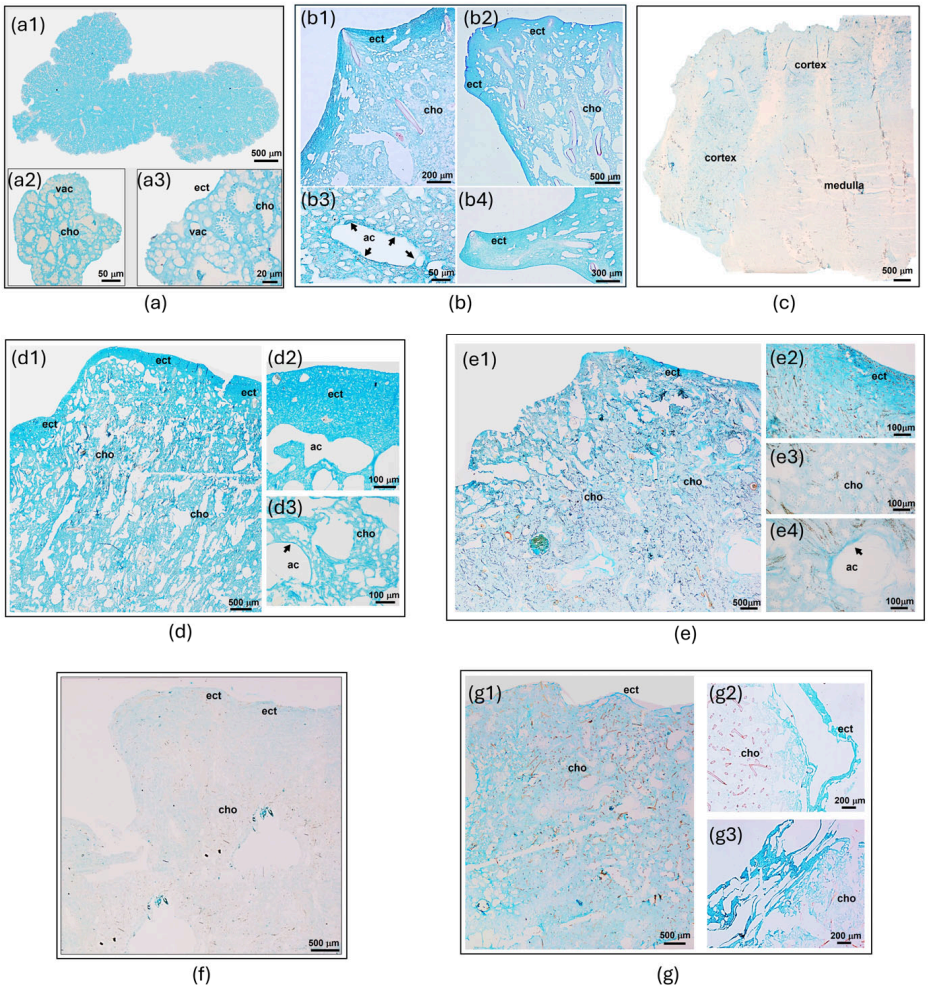


Figure 3. General view and some details of histological sections of the studied sponges. (**a**) *Oscarella lobularis*: general view of a sponge bud showing the uniformity of stain (**a1**); two different magnifications of the outer region composed by a thin ectosome and vacuolated cells, and the choanosome (inner region) containing choanocytes (**a2**,**a3**). (**b**) *Aplysina aerophoba*: general view of the mother sponge (**b1**) and of the pedunculated buds (**b2**,**b4**); the ECM shows a higher content of APs in the ectosome (**b2**,**b4**) contrasting with the moderately stained choanosome, in which APs line the canal wall of the aquiferous system ((**b3**), black arrows). The fibrous skeleton is visible with a light pinkish outline (**b1**,**b2**). (**c**) *Tethya aurantium* transverse body section: the cortex displays weak staining, while the medulla appears almost unstained. (**d**) *Ircinia retidermata*: general view of the sponge body showing a robust ectosome (outermost layer) densely stained and a choanosome (inner region) traversed by numerous canals of the aquiferous system (**d1**,**d2**), making the tissue less compact than the ectosome and resulting in less intense staining, except for the aquiferous canals wall rich in AP and well stained ((**d3**) black arrow). (**e**) *Sarcotragus spinosulus*: general view of the sponge body showing a high concentration of APs in the ectosome, more intensely stained than the choanosome (**e1**–**e3**), and well-stained ECM surrounding the canals of the inner choanosome ((**e4**), black arrow). (**f**) *Crambe crambe*: general view highlighting a very low staining intensity, although a slight difference between the ectosome and the choanosome can be observed. (**g**) *Hippospongia communis*: general view of the sponge body highlighting a thin, densely stained ectosome (outermost layer) and a faintly stained choanosome, with more evident AP content lining the canals and cavities of the aquiferous system (**g1**); details of the outer choanosome (blue–turquoise), highlighting the lined canals and cavities of the aquiferous system within the ECM (**g2**,**g3**). The fibrous skeleton, negative to the stain, is delineated by inorganic inclusions (**g1**,**g2**). Abbreviations: ect: ectosome; cho: choanosome; ac: aquiferous canals; vac: vacuolated cells.

In *A. aerophoba*, *I. retidermata*, *S. spinosulus*, and *H. communis*, the ectosome was consistently more intensely stained than the choanosome (Figure 3). In the choanosome of these species, APs were prominently localized in the thickness of the canal and cavity walls of the choanosomal aquiferous system, exhibiting an intense staining in the luminal surfaces (Figure 3b3,d3,e4,g3). In contrast, skeletal elements were generally unstained, although their structural organization remained clearly discernible.

Tethya aurantium and *C. crambe* displayed overall weak Alcian blue reactivity, suggesting comparatively lower amounts of APs within the ECM. In *T. aurantium*, staining was faint in the cortex and nearly absent in the medulla, whereas *C. crambe* showed uniformly low intensity with only a slight ectosome–choanosome differentiation.

Overall, the results identify three staining intensity patterns:

(i). Strongly positive species, characterized by abundant acidic ECM components, i.e., *O. lobularis*, *A. aerophoba*, *I. retidermata*, *S. spinosulus*;

(ii). Moderately stained species, with localized enrichment primarily in the ectosome and aquiferous canals, i.e., *H. communis*;

(iii). Weakly stained species, exhibiting limited Alcian blue reactivity, i.e., *T. aurantium*, *C. crambe*.

The observed gradient of staining intensity across species is consistent with differences in ECM composition and organization, density and structural arrangement, relative abundance of APs, and interspecific variation in Alcian blue affinity.

3.2. Biochemical Analyses

Low-pressure anion-exchange chromatography, a classical GAGs purification technique, was applied for the fractionation of APs extracted by proteolytic treatment with papain from specimens of seven experimental model species. Each fraction was assessed for hexuronic acid content, whereas the most abundant ones were resolved by carbohydrate electrophoresis and evaluated for susceptibility to depolymerization with specific lyases.

3.2.1. Hexuronic Acid Content

As reported in Table 2, the total yield of UA-containing polysaccharides isolated from the studied sponges ranged from about 1600 µg/g DDT in *T. aurantium* and *A. aerophoba*, to about 3100 µg/g DDT in *O. lobularis* and *H. communis*. Notably, about 98% of these UA-containing polysaccharides were found in the first and second elution, with a remarkable variability spanning from *T. aurantium*, in which the first elution was the most abundant (94%), to *I. retidermata*, in which the UA content was equally distributed. The following qualitative and functional analyses were performed on these two fractions.

Table 2. Hexuronic acid content in each fraction obtained from the seven investigated sponge species.

	O. lobularis		***A. aerophoba***		***T. aurantium***		***I. retidermata***		***S. spinosulus***		***C. crambe***		***H. communis***	
	µg/gDDT	**%**	**µg/gDDT**	**%**	**µg/gDDT**	**%**	**µg/gDDT**	**%**	**µg/gDDT**	**%**	**µg/gDDT**	**%**	**µg/gDDT**	**%**
IE	2222.88	71.11	989.93	62.17	1509.68	94.12	1097.57	47.30	1652.78	65.54	2021.32	86.90	1860.67	59.80
IIE	848.52	27.14	549.40	34.51	63.09	3.93	1157.48	49.88	779.17	30.90	252.57	10.86	1162.21	37.35
IIIE	39.20	1.25	38.18	2.40	18.08	1.13	50.95	2.20	69.63	2.76	41.04	1.76	50.56	1.62
IVE	15.53	0.50	14.66	0.92	13.22	0.82	14.36	0.62	20.30	0.80	11.00	0.47	38.11	1.22
Total	3126.14		1592.17		1604.07		2320.37		2521.87		2325.94		3111.55	

3.2.2. Electrophoretic Profiles

Carbohydrate electrophoresis allows for the separation of APs based on both molecular masses and charge densities, which are specifically stained from blue to purple to yellow as the degree of sulfation increases, thanks to the metachromasia phenomenon of the

cationic carbocyanine dye Stains-all [29]. Similarly to standard DS and Hep, both the first and the second elution of each species show polysaccharides with a wide range of molecular weights, as evidenced by smeared lanes (Figure 4). The smeared profile was not evident for standard HA, which, although heterogeneous in terms of molecular weight (1,500,000–1,750,000 Da), was too big to be resolved in the adopted gel system. Concerning the staining, the first elutions showed predominantly blue (except for *O. lobularis* in which it was purple), similarly to HA, whereas the second elutions were purple (except for *O. lobularis* in which the central part was red and the lower part yellow, similarly to DS and the highly sulfated Hep, respectively), suggesting a higher degree of sulfation, according with the ionic strength (1 M NaCl) used to detach the AP constituents from the stationary phase of the column chromatography (Figure 4). Although C-PAGE is not a quantitative method, few qualitative-quantitative considerations can be made. In particular, while equal quantities, in terms of UA, were loaded for each sample, some differences were evidenced from the electrophoretic profiles. In fact, both elutions from *T. aurantium* and *C. crambe* showed quite faint, suggesting low quantities of loaded APs. Conversely, *A. aerophoba*, *I. retidermata*, *S. spinosulus* and *H. communis* showed quite intense first elutions as well as second elutions characterized by dark, thick bands in the upper part of the gel (cathodic end), overall indicative of higher loading. With regard to *O. lobularis*, the high degree of sulfation of both fractions could be responsible for the intense Alcian Blue staining, which is primarily due to electrostatic linkages with anionic carboxyl and sulfate groups. These observations may explain some emerging inconsistencies by comparing the staining of histological sections and the hexuronic acid tissue concentration, suggesting that the latter is not representative of the overall AP content in these species.

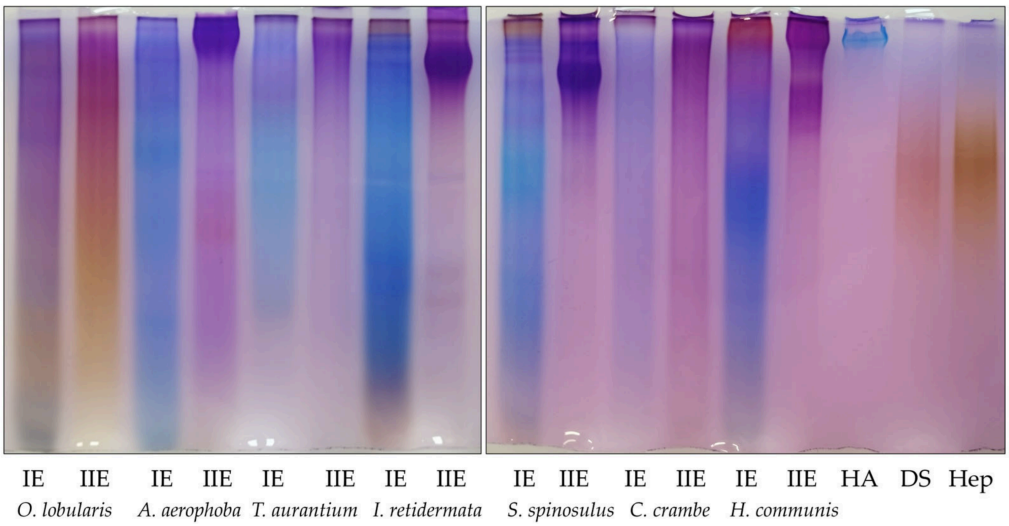


Figure 4. Electrophoretic profiles of the first and second elutions (IE and IIE) from the seven sponge species and standard GAGs, namely high-molecular-weight hyaluronic acid (HA), dermatan sulfate (DS), and heparin (Hep).

From a taxonomic perspective, the electrophoretic profiles revealed marked interspecific heterogeneity. Indeed, *I. retidermata* and *S. spinosulus* (Family Irciniidae, Order Dictyoceratida) showed similar electrophoretic profiles, in accordance with their close systematic relationship [30]. In contrast, *H. communis* (Family Spongiidae, Order Dictyoceratida) exhibited a clearly distinct pattern. A different trend emerged for *T. aurantium* and *C. crambe*. These species of the subclass Heteroscleromorpha belong to different orders; nevertheless, they showed comparable electrophoretic patterns. Overall, these observations suggest that the electrophoretic profiles may be sensitive to taxonomic structure at multiple

hierarchical levels, thus representing a potentially valuable support to morphological and molecular data for improving phylogenetic resolution within Porifera.

Both the first and the second elutions from each species under study, as well as the standard GAGs, were subjected to treatment with specific lyases known to be effective on GAGs from vertebrates. As shown for *S. spinosulus* (Figure 5), neither the first nor the second elution of any species was susceptible to depolymerization by chondroitin ABC lyase (Figure 5a), which was instead effective on both standard HA and DS, or by hyaluronidase (Figure 5b), this latter effective only on standard HA.

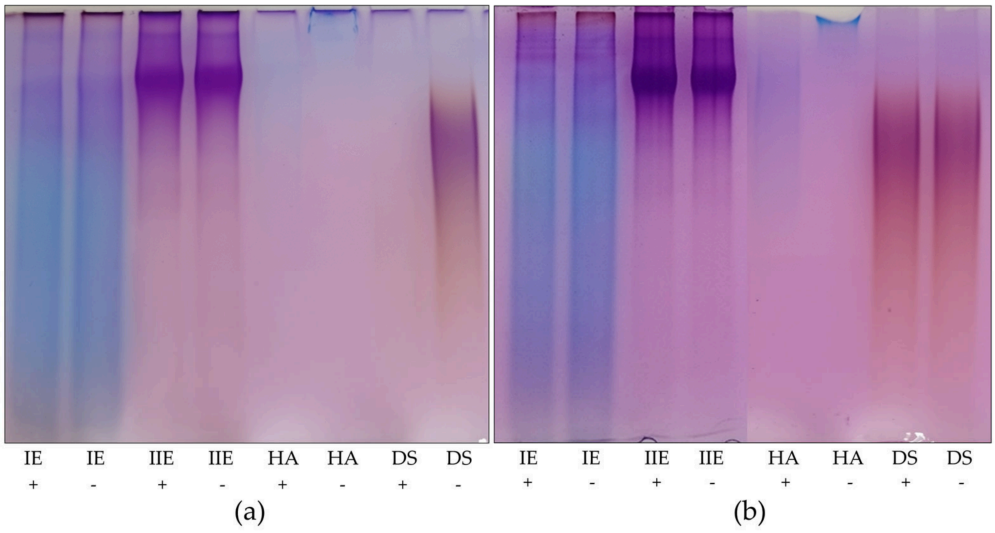


Figure 5. Electrophoretic profiles of the first and second elutions (IE and IIE) from the sponge *S. spinosulus* and standard GAGs, namely high-molecular-weight hyaluronic acid (HA), dermatan sulfate (DS), before (-) and after (+) chondroitin ABC lyase (panel (**a**)) or hyaluronidase (panel (**b**)) treatment.

3.2.3. Anticoagulant Activity of Purified Polysaccharide Fractions

The first and second fractions from the species investigated were assessed, in vitro, for their potential inhibitory activity towards the coagulation cascade. In particular, the effects on the intrinsic, extrinsic, and common pathways of the coagulation were evaluated using activated partial thromboplastin time (aPTT), prothrombin time (PT), and thrombin time (TT) assays, respectively, compared with standard GAGs, namely HA, DS and Hep, the latter being a positive control for each assay (Table 3, Figure 6). In fact, it is known that Hep exerts its primary anticoagulant effect by inactivating factor Xa and thrombin, part of the common pathway of coagulation through a mechanism dependent on antithrombin (AT). It binds to AT via a high-affinity pentasaccharide sequence found on approximately one-third of heparin molecules. Through the inactivation of thrombin, heparin serves a dual purpose, preventing fibrin formation and suppressing thrombin-mediated platelet activation, as well as the activation of factors V and VIII of the intrinsic pathway [31,32].

As previously shown, data concerning standard GAGs confirmed that Hep was the most effective polysaccharide in inhibiting clot formation in each assay, whereas low or no effects were evidenced for DS and HA, respectively [14]. Among the species analyzed, the first and the second fractions from both *T. aurantium* and *C. crambe* showed no or weak in vitro effects on coagulation. All the second elutions of the other species showed a strong inhibitory effect on both aPTT and TT, comparable to Hep. Concerning aPTT, *I. retidermata* and *H. communis* reached the endpoint of 300 s at both 5 and 10 μgUA/mL, whereas *S. spinosulus*, *O. lobularis*, and *A. aerophoba* reached it at 10 μgUA/mL. With reference to TT, *A. aerophoba*, *I. retidermata*, *S. spinosulus* and *H. communis* had similar effects on coagulation

time with respect to Hep (endpoint at 5 µgUA/mL), whereas *O. lobularis* was less effective at the lowest concentrations, reaching the endpoint at 100 µgUA/mL. These effects could be attributed, at least in part, to the highly dispersed highly sulfated APs found in *O. lobularis*, and to the APs shown as dark, thick bands in *A. aerophoba*, *I. retidermata*, *S. spinosulus*, and *H. communis*, by C-PAGE.

Table 3. Comparative effects of the first and second fractions from the investigated species, as well as standard GAGs, on intrinsic (aPTT assay), extrinsic (PT assay) and common (TT assay) pathways of coagulation. The number of checkmarks reported refers to the prolongation of coagulation time induced by the first and second elutions (IE and IIE) with respect to Hep. ✓, inhibitory effect on coagulation; X, no effect on coagulation.

		O. lobularis	*A. aerophoba*	*T. aurantium*	*I. retidermata*	*S. spinosulus*	*C. crambe*	*H. communis*	HA	DS	Hep
aPTT	**IE**	✓✓✓	✓	X	X	✓	X	✓✓	X	✓	✓✓✓✓✓
	IIE	✓✓	✓✓	X	✓✓✓	✓✓	✓	✓✓✓			
PT	**IE**	X	X	X	X	X	X	X	X	X	✓✓✓
	IIE	✓✓✓	✓	X	✓✓✓	✓✓	X	X			
TT	**IE**	✓✓✓	✓	X	X	✓✓	X	✓✓✓	X	✓✓	✓✓✓✓✓
	IIE	✓✓✓	✓✓✓✓✓	X	✓✓✓✓✓	✓✓✓✓✓	✓	✓✓✓✓✓			

Also, the first elutions of both *O. lobularis* and *H. communis* were effective in prolonging aPTT and TT, probably due to a sulfated component, evident throughout all the lane in *O. lobularis* as well as in the upper part of the lane in *H. communis*. Indeed, it is known that the anticoagulant potency of marine sulfated polysaccharides (MSPs) depends on their structural characteristics, most notably the degree and pattern of sulfation [33]. While a higher sulfate content broadly correlates with greater anticoagulant activity, the precise positioning of sulfate groups on individual sugar residues is equally important. Molecular weight further shapes this activity, with higher molecular weight fractions resulting in stronger anticoagulant effects, which is reduced by depolymerization [33].

Notably, *O. lobularis* (Homoscleromorpha) exhibits distinctive electrophoretic profiles for both elutions, as well as a strong inhibitory effect on both aPTT and TT, which clearly differentiate it from the other species. Interestingly, members of Homoscleromorpha possess epithelial-like tissues with a true basement membrane, a condition that is exceptional among sponges [22,34]. In addition, their molecular and biochemical profiles reveal similarities that distinguish them from other Porifera lineages [35]. Phylogenetic analyses based on molecular data further support the hypothesis that this group occupies a position relatively closer to the eumetazoan clade, particularly the Bilateria [36–38]. Collectively, these histological, chemical, and genetic characteristics contribute to the interpretation of *O. lobularis* as a taxon of considerable evolutionary significance in discussions concerning early metazoan diversification [34].

There were almost no effects on PT, except for the second elutions of *O. lobularis*, *I. retidermata* and *S. spinosulus*. In this respect, dedicated studies of direct thrombin inhibitors show very different concentration–response curves for PT vs. TT, with TT typically much more responsive than PT, which may be only modestly prolonged or even stay within near-normal range [39,40].

Our results show, for the first time, that the most primitive metazoans on the evolutionary scale own APs in their ECM with interesting anticoagulant properties, in line with current knowledge on the mechanisms of coagulation pathway inhibition by some MSPs from other marine invertebrate taxa [33]. In this regard, they are known to exert anticoagulant effects, chiefly by enhancing the activity of serpin inhibitors, namely antithrombin III (ATIII) and heparin cofactor II (HCII), thereby accelerating the inhibition

of thrombin (factor IIa) and factor Xa within the common coagulation pathway [41–43]. Furthermore, some of them are known to enhance plasminogen activation, contributing to thrombolytic activity and clot breakdown [44,45]. In addition, some sulfated galactoarabinans and arabinogalactans from green algae have been reported to strongly inhibit factors of the intrinsic pathway of coagulation (XII, XI, IX, VIII) [46–48]. Although initial binding is driven primarily by electrostatic interactions, the specific recognition and regulation of target proteins are determined by the stereochemical characteristics of the polysaccharide, including the degree and pattern of sulfation, as well as backbone structure [47].

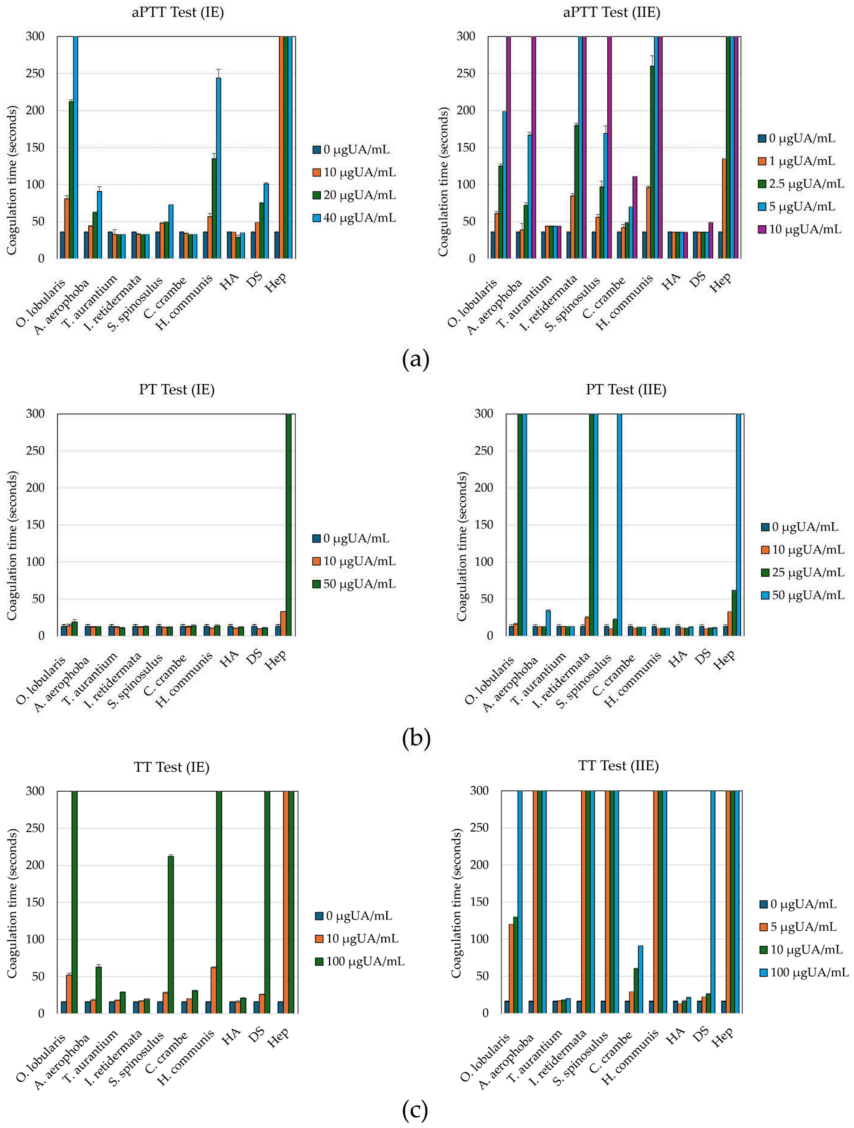


Figure 6. In vitro anticoagulant activities of the first (left panels) and second (right panels) fractions from the investigated species, as well as standard GAGs, namely high-molecular-weight hyaluronic acid (HA), dermatan sulfate (DS), and heparin (Hep), evaluated by aPTT (**a**), PT (**b**), and TT (**c**) assays. Values are reported as mean ± SD.

Several in vitro and in vivo studies reported low toxicity and good cell compatibility for MSPs, establishing a strong safety profile for biomedical use [16,49]. In this respect, we previously reported no negative effects for the APs purified from *S. spinosulus* on in vitro metabolic activity of human fibroblasts grown for seven days in culture [14]. These properties, combined with their structural and functional versatility, position MSPs as compelling alternatives to conventional anticoagulants for next-generation anticoagulant

therapies, as well as smart functionalization agents for tissue engineering applications. Integrating detailed structural knowledge with functional studies will be key to overcoming translational barriers and fully realizing their therapeutic promise.

4. Conclusions

In this study, a screening of several phylogenetically distant Mediterranean Porifera species for the presence of potentially interesting anticoagulant polysaccharide species was performed. The sponges *Oscarella lobularis*, *Ircinia retidermata*, *Sarcotragus spinosulus*, *Hippospongia communis*, and *Aplysina aerophoba* showed APs with a strong inhibitory effect on both intrinsic and common pathways of coagulation comparable to heparin, which was used as standard.

This finding represents a preliminary mandatory step in selecting the most promising candidates for deep structural characterization. Usually performed on milligram-scale quantities of material by Fourier Transform Infrared Spectroscopy and Nuclear Magnetic Resonance Spectroscopy, this analysis would provide insights into the anticoagulant properties described from a mechanistic point of view.

Our findings on Porifera reinforce and extend the current paradigm derived from other marine invertebrates and algae, confirming that MSPs represent an evolutionarily conserved class of bioactive polysaccharides with potent hemostasis-modulating properties. Taken together, these preliminary data suggest MSPs from basal metazoans are promising candidates for next-generation anticoagulant agents, with potential applications in regenerative medicine and tissue engineering. Future efforts should focus on detailed structural characterization, standardized functional assays, and in vivo efficacy and safety studies to bridge the gap between basic research and clinical translation to fully exploit their therapeutic potential. Along with the feasibility of rearing these organisms in an environmentally sustainable way, this approach links biomedical innovation with environmental stewardship, encouraging the responsible use of marine biodiversity in accordance with blue economy principles.

Author Contributions: Conceptualization: T.C. and A.J.L.; methodology: G.C., T.C. and A.J.L.; validation: G.C. and G.N.; formal analysis: T.C. and A.J.L.; investigation: T.C. and A.J.L.; resources: N.F., M.F. and A.J.L.; data curation: T.C., G.C., G.N. and A.J.L.; writing—original draft: T.C. and A.J.L.; writing—review and editing: T.C., G.C., G.N., P.M., N.F., R.M., M.F. and A.J.L.; supervision: M.F. and A.J.L.; project administration: A.J.L.; funding acquisition: M.F. and A.J.L. All authors have read and agreed to the published version of the manuscript.

Funding: This research received no external funding.

Institutional Review Board Statement: Ethical approval was provided by the Organismo Preposto al Benessere e alla Sperimentazione Animale (OPBSA) of the University of Sassari (Prot. No. 33739, dated 26 March 2026).

Informed Consent Statement: Not applicable.

Data Availability Statement: The data presented in this work are available from the lead contact upon request.

Acknowledgments: This work was supported by the European Union—NextGenerationEU (DM 737/2021, RISORSE 2021–2022, 2022–2023 [CUP J55F21004240001]). Authors are grateful to the staff of the Club Nautico Capo Caccia and the Capo Caccia—Isola Piana Marine Protected Area for their kind and key support in the field.

Conflicts of Interest: The authors declare no conflicts of interest.

Abbreviations

The following abbreviations are used in this manuscript:

ECM	Extracellular matrix
APs	Acidic polysaccharides
UFH	Unfractionated heparin
LMWH	Low-molecular-weight heparin
FCS	Fucosylated chondroitin sulfate
aPTT	Activated partial thromboplastin time
PT	Prothrombin time
TT	Thrombin time
DDT	Dehydrated and delipidated tissues
DEAE-	Diethylaminoethyl-
UA	Uronic acid/Hexuronic acid
C-PAGE	Carbohydrate polyacrylamide gel electrophoresis
HMW-HA	High molecular weight hyaluronic acid
DS	Dermatan sulfate
Hep	Heparin
GAGs	Glycosaminoglycans
MSPs	Marine sulfated polysaccharides

References

1. Garcia, D.A.; Baglin, T.P.; Weitz, J.I.; Samama, M.M. Parenteral Anticoagulants: Antithrombotic Therapy and Prevention of Thrombosis, 9th Ed: American College of Chest Physicians Evidence-Based Clinical Practice Guidelines. *Chest* **2012**, *141*, e24S–e43S. [CrossRef] [PubMed]
2. Alban, S. Adverse Effects of Heparin. *Handb. Exp. Pharmacol.* **2012**, 211–263. [CrossRef]
3. Han, G.; Song, S.; Wan, S.; Wang, M.; Zhou, D.; Ji, X.; Meng, R. Heparin-Induced Thrombocytopenia and Thrombosis in Patients With or Without a Thrombophilia Background: A Systematic Review Involved 602 Cases. *Int. J. Vasc. Med.* **2025**, *2025*, 9338124. [CrossRef] [PubMed]
4. Castelli, R.; Cassinerio, E.; Cappellini, M.D.; Porro, F.; Graziadei, G.; Fabris, F. Heparin Induced Thrombocytopenia: Pathogenetic, Clinical, Diagnostic and Therapeutic Aspects. *Cardiovasc. Hematol. Disord. Drug Targets* **2007**, *7*, 153–162. [CrossRef]
5. Chandika, P.; Tennakoon, P.; Kim, T.-H.; Kim, S.-C.; Je, J.-Y.; Kim, J.-I.; Lee, B.; Ryu, B.; Kang, H.W.; Kim, H.-W.; et al. Marine Biological Macromolecules and Chemically Modified Macromolecules; Potential Anticoagulants. *Mar. Drugs* **2022**, *20*, 654. [CrossRef]
6. Ning, Z.; Wang, P.; Zuo, Z.; Tao, X.; Gao, L.; Xu, C.; Wang, Z.; Wu, B.; Gao, N.; Zhao, J. A Fucan Sulfate with Pentasaccharide Repeating Units from the Sea Cucumber *Holothuria floridana* and Its Anticoagulant Activity. *Mar. Drugs* **2022**, *20*, 377. [CrossRef]
7. Luthuli, S.; Wu, S.; Cheng, Y.; Zheng, X.; Wu, M.; Tong, H. Therapeutic Effects of Fucoidan: A Review on Recent Studies. *Mar. Drugs* **2019**, *17*, 487. [CrossRef]
8. Felix, A.L.; Penno, S.M.; Bezerra, F.F.; Mourão, P.A.S. Fucosylated Chondroitin Sulfate, an Intriguing Polysaccharide from Sea Cucumber: Past, Present, and Future. *Glycobiology* **2025**, *35*, cwae098. [CrossRef]
9. Xiao, C.; Zhao, L.; Gao, N.; Wu, M.; Zhao, J. Nonasaccharide Inhibits Intrinsic Factor Xase Complex by Binding to Factor IXa and Disrupting Factor IXa-Factor VIIIa Interactions. *Thromb. Haemost.* **2019**, *119*, 705–715. [CrossRef]
10. Manconi, R.; Cubeddu, T.; Pronzato, R.; Sanna, M.A.; Nieddu, G.; Gaino, E.; Stocchino, G.A. Collagenic Architecture and Morphotraits in a Marine Basal Metazoan as a Model for Bioinspired Applied Research. *J. Morphol.* **2022**, *283*, 585–604. [CrossRef]
11. Langasco, R.; Cadeddu, B.; Formato, M.; Lepedda, A.J.; Cossu, M.; Giunchedi, P.; Pronzato, R.; Rassu, G.; Manconi, R.; Gavini, E. Natural Collagenic Skeleton of Marine Sponges in Pharmaceutics: Innovative Biomaterial for Topical Drug Delivery. *Mater. Sci. Eng. C Mater. Biol. Appl.* **2017**, *70*, 710–720. [CrossRef]
12. Ehrlich, H.; Litowczenko, J.; Szczurek, A.; Voronkina, A.; Pakuła, D.; Frydrych, M.; Przekop, R.E.; Smirnov, I.; Petrov, S.; Sieliverstov, I.; et al. 3D Skeletal Scaffolds of Marine Keratosan Demosponges Origin as Renewable Sources for Bioinspiration in Modern Structural Biomimetics and Tissue Engineering. *Biomimetics* **2026**, *11*, 124. [CrossRef] [PubMed]
13. Ledda, F.D.; Pronzato, R.; Manconi, R. Mariculture for Bacterial and Organic Waste Removal: A Field Study of Sponge Filtering Activity in Experimental Farming. *Aquac. Res.* **2014**, *45*, 1389–1401. [CrossRef]

14. Nieddu, G.; Obino, G.; Ciampelli, C.; Brunetti, A.; Cubeddu, T.; Manconi, R.; Stocchino, G.A.; Deiana, G.A.; Formato, M.; Lepedda, A.J. Purification of an Acidic Polysaccharide with Anticoagulant Activity from the Marine Sponge *Sarcotragus spinosulus*. *Mar. Drugs* **2024**, *22*, 139. [CrossRef] [PubMed]
15. Obino, G.; Nieddu, G.; Nagy, M.; Ippel, H.; Cubeddu, T.; Spronk, H.M.H.; Hackeng, T.M.; Formato, M.; Lepedda, A.J.; Moroni, L. Marine-Derived Sulfated Polysaccharides Enhance Hemocompatibility and Endothelialization of Nanofibrous PCL for Vascular Graft Applications. *Cell Biomater.* **2025**, *1*, 100155. [CrossRef]
16. Obino, G.; Sensini, A.; Ten Brink, T.; Nieddu, G.; Bodet, T.; Deiana, G.A.; van Griensven, M.; Formato, M.; Lepedda, A.J.; Moroni, L. Tunable Bioresorbable Scaffolds With Marine Sulfated Polysaccharides for Small-Caliber Vascular Grafts: A Multi-Layered Strategy Combining Electrospinning and 4-Axis Printing. *Adv. Healthc. Mater.* **2026**, *2*, e05314. [CrossRef]
17. Zierer, M.S.; Mourão, P.A. A Wide Diversity of Sulfated Polysaccharides Are Synthesized by Different Species of Marine Sponges. *Carbohydr. Res.* **2000**, *328*, 209–216. [CrossRef]
18. Misevic, G.N.; Guerardel, Y.; Sumanovski, L.T.; Slomianny, M.-C.; Demarty, M.; Ripoll, C.; Karamanos, Y.; Maes, E.; Popescu, O.; Strecker, G. Molecular Recognition between Glyconectins as an Adhesion Self-Assembly Pathway to Multicellularity. *J. Biol. Chem.* **2004**, *279*, 15579–15590. [CrossRef]
19. Vilanova, E.; Coutinho, C.C.; Mourão, P.A.S. Sulfated Polysaccharides from Marine Sponges (Porifera): An Ancestor Cell-Cell Adhesion Event Based on the Carbohydrate-Carbohydrate Interaction. *Glycobiology* **2009**, *19*, 860–867. [CrossRef]
20. Pérez-López, P.; Ledda, F.D.; Bisio, A.; Feijoo, G.; Perino, E.; Pronzato, R.; Manconi, R.; Moreira, M.T. Life Cycle Assessment of in Situ Mariculture in the Mediterranean Sea for the Production of Bioactive Compounds from the Sponge *Sarcotragus spinosulus*. *J. Clean. Prod.* **2017**, *142*, 4356–4368. [CrossRef]
21. Padiglia, A.; Ledda, F.D.; Padedda, B.M.; Pronzato, R.; Manconi, R. Long-Term Experimental in Situ Farming of Crambe Crambe (Demospongiae: Poecilosclerida). *PeerJ* **2018**, *6*, e4964. [CrossRef] [PubMed]
22. Ereskovsky, A.V.; Borisenko, I.E.; Lapébie, P.; Gazave, E.; Tokina, D.B.; Borchiellini, C. *Oscarella lobularis* (Homoscleromorpha, Porifera) Regeneration: Epithelial Morphogenesis and Metaplasia. *PLoS ONE* **2015**, *10*, e0134566. [CrossRef] [PubMed]
23. Gazave, E.; Lapébie, P.; Renard, E.; Vacelet, J.; Rocher, C.; Ereskovsky, A.V.; Lavrov, D.V.; Borchiellini, C. Molecular Phylogeny Restores the Supra-Generic Subdivision of Homoscleromorph Sponges (Porifera, Homoscleromorpha). *PLoS ONE* **2010**, *5*, e14290. [CrossRef] [PubMed]
24. Sipkema, D.; Franssen, M.C.R.; Osinga, R.; Tramper, J.; Wijffels, R.H. Marine Sponges as Pharmacy. *Mar. Biotechnol.* **2005**, *7*, 142–162. [CrossRef]
25. Müller, W.E.G.; Schröder, H.C.; Wiens, M.; Perović-Ottstadt, S.; Batel, R.; Müller, I.M. Traditional and Modern Biomedical Prospecting: Part II-the Benefits: Approaches for a Sustainable Exploitation of Biodiversity (Secondary Metabolites and Biomaterials from Sponges). *Evid. Based. Complement. Alternat. Med.* **2004**, *1*, 133–144. [CrossRef]
26. Vlachou, P.; Tsafantakis, N.; Milic, N.; Polyzois, A.; Baira, E.; Termentzi, A.; Le Goff, G.; Ouazzani, J.; Fokialakis, N. Chemical Investigation of the Mediterranean Sponge Crambe Crambe by UHPLC-HRMS/MS via Manual and Computational Dereplication Approaches. *Mar. Drugs* **2024**, *22*, 522. [CrossRef]
27. Bondu, S.; Genta-Jouve, G.; Leirós, M.; Vale, C.; Guigonis, J.-M.; Botana, L.M.; Thomas, O.P. Additional Bioactive Guanidine Alkaloids from the Mediterranean Sponge Crambe Crambe. *RSC Adv.* **2012**, *2*, 2828. [CrossRef]
28. Bitter, T.; Muir, H.M. A Modified Uronic Acid Carbazole Reaction. *Anal. Biochem.* **1962**, *4*, 330–334. [CrossRef]
29. Andrade, J.P.S.; Oliveira, C.P.; Tovar, A.M.F.; Mourão, P.A.d.S.; Vilanova, E. A Color-Code for Glycosaminoglycans Identification by Means of Polyacrylamide Gel Electrophoresis Stained with the Cationic Carbocyanine Dye Stains-All. *Electrophoresis* **2018**, *39*, 666–669. [CrossRef]
30. Hardoim, C.C.P.; Esteves, A.I.S.; Pires, F.R.; Gonçalves, J.M.S.; Cox, C.J.; Xavier, J.R.; Costa, R. Phylogenetically and Spatially Close Marine Sponges Harbour Divergent Bacterial Communities. *PLoS ONE* **2012**, *7*, e53029. [CrossRef]
31. Hirsh, J.; Anand, S.S.; Halperin, J.L.; Fuster, V. Mechanism of Action and Pharmacology of Unfractionated Heparin. *Arterioscler. Thromb. Vasc. Biol.* **2001**, *21*, 1094–1096. [CrossRef]
32. Olson, S.T.; Richard, B.; Izaguirre, G.; Schedin-Weiss, S.; Gettins, P.G.W. Molecular Mechanisms of Antithrombin-Heparin Regulation of Blood Clotting Proteinases. A Paradigm for Understanding Proteinase Regulation by Serpin Family Protein Proteinase Inhibitors. *Biochimie* **2010**, *92*, 1587–1596. [CrossRef]
33. Li, K.; Li, R.; Liu, Y.; Li, G.; Liu, S. Diversity, Mechanism and Structure-Activity Relationships of Marine Anticoagulant-Active Polysaccharides: A Review. *Int. J. Biol. Macromol.* **2025**, *306*, 141742. [CrossRef] [PubMed]
34. Boury-Esnault, N.; Lavrov, D.V.; Ruiz, C.A.; Perez, T. The Integrative Taxonomic Approach Applied to Porifera: A Case Study of the Homoscleromorpha. *Integr. Comp. Biol.* **2013**, *53*, 416–427. [CrossRef] [PubMed]
35. Lapébie, P.; Gazave, E.; Ereskovsky, A.; Derelle, R.; Bézac, C.; Renard, E.; Houliston, E.; Borchiellini, C. WNT/Beta-Catenin Signalling and Epithelial Patterning in the Homoscleromorph Sponge *Oscarella*. *PLoS ONE* **2009**, *4*, e5823. [CrossRef]

36. Rocher, C.; Vernale, A.; Fierro-Constaín, L.; Séjourné, N.; Chenesseau, S.; Marschal, C.; Issartel, J.; Le Goff, E.; Stroebel, D.; Jouvion, J.; et al. The Buds of *Oscarella lobularis* (Porifera, Homoscleromorpha): A New Convenient Model for Sponge Cell and Evolutionary Developmental Biology. *J. Exp. Zool. B Mol. Dev. Evol.* **2024**, *342*, 503–528. [CrossRef] [PubMed]
37. Wang, X.; Lavrov, D. V Mitochondrial Genome of the Homoscleromorph *Oscarella carmela* (Porifera, Demospongiae) Reveals Unexpected Complexity in the Common Ancestor of Sponges and Other Animals. *Mol. Biol. Evol.* **2007**, *24*, 363–373. [CrossRef]
38. Wörheide, G.; Dohrmann, M.; Erpenbeck, D.; Larroux, C.; Maldonado, M.; Voigt, O.; Borchiellini, C.; Lavrov, D.V. Deep Phylogeny and Evolution of Sponges (Phylum Porifera). *Adv. Mar. Biol.* **2012**, *61*, 1–78.
39. Curvers, J.; van de Kerkhof, D.; Stroobants, A.K.; van den Dool, E.-J.; Scharnhorst, V. Measuring Direct Thrombin Inhibitors with Routine and Dedicated Coagulation Assays: Which Assay Is Helpful? *Am. J. Clin. Pathol.* **2012**, *138*, 551–558. [CrossRef]
40. Sivaraja, M.; Pozzi, N.; Rienzo, M.; Lin, K.; Shiau, T.P.; Clemens, D.M.; Igoudin, L.; Zalicki, P.; Chang, S.S.; Estiarte, M.A.; et al. Reversible Covalent Direct Thrombin Inhibitors. *PLoS ONE* **2018**, *13*, e0201377. [CrossRef]
41. Zhang, W.; Jin, W.; Pomin, V.H.; Zhang, F.; Linhardt, R.J. Interactions of Marine Sulfated Glycans with Antithrombin and Platelet Factor 4. *Front. Mol. Biosci.* **2022**, *9*, 954752. [CrossRef] [PubMed]
42. Ustyuzhanina, N.E.; Bilan, M.I.; Dmitrenok, A.S.; Borodina, E.Y.; Stonik, V.A.; Nifantiev, N.E.; Usov, A.I. A Highly Regular Fucosylated Chondroitin Sulfate from the Sea Cucumber *Massinium magnum*: Structure and Effects on Coagulation. *Carbohydr. Polym.* **2017**, *167*, 20–26. [CrossRef] [PubMed]
43. Chen, S.; Li, G.; Wu, N.; Guo, X.; Liao, N.; Ye, X.; Liu, D.; Xue, C.; Chai, W. Sulfation Pattern of the Fucose Branch Is Important for the Anticoagulant and Antithrombotic Activities of Fucosylated Chondroitin Sulfates. *Biochim. Biophys. Acta* **2013**, *1830*, 3054–3066. [CrossRef] [PubMed]
44. Liu, X.; Du, P.; Liu, X.; Cao, S.; Qin, L.; He, M.; He, X.; Mao, W. Anticoagulant Properties of a Green Algal Rhamnan-Type Sulfated Polysaccharide and Its Low-Molecular-Weight Fragments Prepared by Mild Acid Degradation. *Mar. Drugs* **2018**, *16*, 445. [CrossRef]
45. Chen, Q.; Zhang, M.; Liu, Y.; Liu, W.; Peng, C.; Zheng, L. Sulfated Polysaccharides with Anticoagulant Potential: A Review Focusing on Structure-Activity Relationship and Action Mechanism. *Chem. Biodivers.* **2024**, *21*, e202400152. [CrossRef]
46. Cao, S.; He, X.; Qin, L.; He, M.; Yang, Y.; Liu, Z.; Mao, W. Anticoagulant and Antithrombotic Properties in Vitro and in Vivo of a Novel Sulfated Polysaccharide from Marine Green Alga *Monostroma nitidum*. *Mar. Drugs* **2019**, *17*, 247. [CrossRef]
47. He, M.; Yang, Y.; Shao, Z.; Zhang, J.; Feng, C.; Wang, L.; Mao, W. Chemical Structure and Anticoagulant Property of a Novel Sulfated Polysaccharide from the Green Alga *Cladophora oligoclada*. *Mar. Drugs* **2021**, *19*, 554. [CrossRef]
48. Qin, L.; He, M.; Yang, Y.; Fu, Z.; Tang, C.; Shao, Z.; Zhang, J.; Mao, W. Anticoagulant-Active Sulfated Arabinogalactan from *Chaetomorpha linum*: Structural Characterization and Action on Coagulation Factors. *Carbohydr. Polym.* **2020**, *242*, 116394. [CrossRef]
49. Arokiarajan, M.S.; Thirunavukkarasu, R.; Joseph, J.; Ekaterina, O.; Aruni, W. Advance Research in Biomedical Applications on Marine Sulfated Polysaccharide. *Int. J. Biol. Macromol.* **2022**, *194*, 870–881. [CrossRef]

Disclaimer/Publisher's Note: The statements, opinions and data contained in all publications are solely those of the individual author(s) and contributor(s) and not of MDPI and/or the editor(s). MDPI and/or the editor(s) disclaim responsibility for any injury to people or property resulting from any ideas, methods, instructions or products referred to in the content.